Modeling tubular shapes in the inner mitochondrial membrane

A Ponnuswamy[1]**, J Nulton**[2]**, J M Mahaffy**[2]**, P Salamon**[2]**, T G Frey**[3] **and A R C Baljon**[1]

[1] Department of Physics, San Diego State University, CA 92182, USA
[2] Department of Mathematics, San Diego State University, CA 92182, USA
[3] Department of Biology, San Diego State University, CA 92182, USA

Abstract
The inner mitochondrial membrane has been shown to have a novel structure that contains tubular components whose radii are of the order of 10 nm as well as comparatively flat regions. The structural organization of mitochondria is important for understanding their functionality. We present a model that can account, thermodynamically, for the observed size of the tubules. The model contains two lipid constituents with different shapes. They are allowed to distribute in such a way that the composition differs on the two sides of the tubular membrane. Our calculations make two predictions: (1) there is a pressure difference of 0.2 atmospheres across the inner membrane as a necessary consequence of the experimentally observed tubule radius of 10 nm, and (2) migration of differently shaped lipids causes concentration variations of the order of 7% between the two sides of the tubular membrane.

1. Introduction

Mitochondria are organelles in eukaryotic cells that provide most of the chemical energy, ATP, from oxidative metabolism. More recently they have been shown to play a key role in apoptosis, or programmed cell death. Mitochondria have their own DNA and are thought to have evolved from a prokaryotic organism that became engulfed and lived inside the ancient eukaryotic cell. Mitochondria have an outer membrane that surrounds a complex inner membrane structure that in turn encloses the matrix space of the organelle. The inner membrane and the matrix contain a rich collection of enzymes that are crucial for breaking down a number of metabolites such as fatty acids and pyruvate-forming Acetyl-CoA. Acetyl-CoA is oxidized via the citric acid cycle to produce reduced nucleotides, NADH and FADH2, that provide reducing potential for the mitochondrial electron transport chain that converts this energy into an electrochemical proton gradient across the inner mitochondrial membrane (IMM). The ATP Synthase uses the proton gradient to synthesize ATP, the principal source of energy for cell function. Mitochondria also interact with the cell in the process of apoptosis. When mitochondria receive certain signals they undergo a structural transformation that leads to

the release of cytochrome c, which in turn causes the cell to destroy itself in a controlled process.

Our research examines the physical structure of mitochondria in the hope of better understanding a number of the key functions performed by this organelle. Electron tomography has provided high resolution three-dimensional structures of 'orthodox' (healthy) mitochondria *in vivo* [1–3]. These structures, shown in figure 1, exhibit several features necessary for proper function. The inner mitochondrial membrane is a protein-rich lipid bilayer membrane with two topological components. (1) An inner boundary membrane (IBM) that lies closely opposed to the outer membrane, and (2) a crista membrane that projects into the matrix, forming cristae, which is either tubular in shape or lamellar. Tubules are connected to the IBM by crista junctions (see figure 1) shaped like the bell of a trumpet [4]. The observed mitochondria have a large matrix volume that pushes the inner boundary membrane against the outer membrane and collapses the cristae into flat lamellar compartments.

In our work, we explore the possibility that at least portions of the mitochondrial membrane make up a thermodynamically stable structure that minimizes free energy [4]. Rather than trying to deduce the morphology from first principles [5], we take the observed morphology as given and
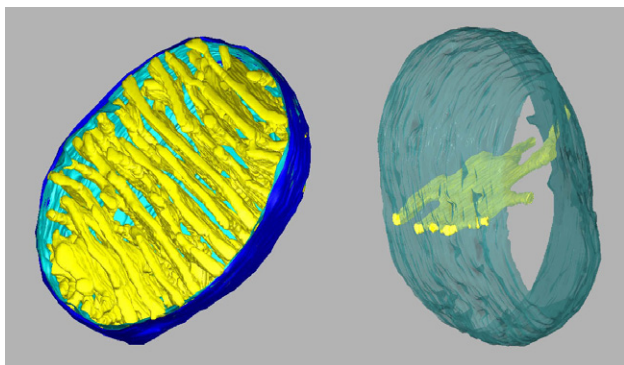
Figure 1. 3D computer models of the mitochondrial membranes generated from the electron tomogram of a mitochondrion observed in chick cerebellum prepared by conventional chemical fixation, dehydration and embedding techniques. The image on the left shows the outer membrane in dark blue, inner boundary membrane in turquoise and all the cristae in yellow. The image on the right shows a typical crista in yellow connected to the inner boundary membrane that has been rendered translucent. The connections are via crista junctions of uniform size and tubular cristae segments of variable length [1–3]. Quicktime movies of 3D models of mitochondria rotating about an axis can be viewed in full color at http://www.sci.sdsu.edu/TFrey/MitoMovie.htm

make inferences regarding the physico-chemical environment in which this morphology could exist.

We begin by noting that the observed morphology shows a definite scale. That the crista junctions have a fairly constant radius of about 10 nm has been noted in several places [1, 4]. In fact, their diameter roughly matches the spacing between the lamellar regions of the cristae and that of the tubules linking these regions to the junctions. It is certainly possible that some skeletal components maintain the spacing everywhere and thereby account for the scale. We consider the hypothesis that such skeletal elements exist only in the lamellae, whose surfaces house the machinery of ATP production, which probably requires (and gives) some mechanical stability at a spacing that roughly matches the distance that the membrane-bound proteins extend into the intermembrane space. In that case the shape of the tubular regions is determined by elastic energy minimization rather than by skeletal elements. Suppose that a cylindrical tubular bilayer of fixed length is constrained in such a way that it can only increase or decrease its radius by exchanging area (molecules) with a flat membrane as a reservoir. It is not surprising, all other things being equal, that its radius would grow indefinitely in order to mitigate the energetic cost of bending required by the formation of the cylindrical tubule. If, however, there was a positive osmotic pressure difference across the membrane, that favors the exterior of the tube, i.e. the mitochondrial matrix, then osmotic work would be required to grow the radius of the tube. The result is a tradeoff of two energetic components (bending and pressure work), giving an equilibrium tube radius whose magnitude depends on the pressure difference. Although such a pressure difference has not been measured, the matrix volume has been shown to respond to changes in osmolarity of the surrounding media [6], and the crista junction diameters respond to changes in matrix volume [7].

The IMM has been shown to contain several types of phospholipids. In addition, 50% of membrane surface is occupied by proteins, which represent approximately 75% of the inner membrane mass. For the sake of simplicity, our model includes no proteins and only the two most common lipid types: phosphatidyl ethanolamine (PE) and phosphatidyl choline (PC). These occur naturally in the IMM at fractions of 27.7% and 44.5%, respectively. Moreover, in our model, we consider only the dioleic acid esters of the lipids DOPE and DOPC, although *in vivo* each is heterogeneous with respect to its fatty acid composition. Although most authors neglect membrane composition altogether, some have attributed the variations in membrane curvature to the existence of domains of differently shaped molecules [8, 10]. Whereas for lipids of limited miscibility [11] these can be seen, we do not expect this to be the case for DOPE and DOPC which are chemically very similar and thus should form nearly ideal solutions in which the entropic incentive to mix is far outweighed by possible energetic advantages of segregation. However, segregation of the lipids according to local membrane curvature is to be expected [12]. We assess the extent to which the geometry of the lipids contributes to the shape of the membrane. The contest here is between the entropic contribution to the free energy and the bending energy savings obtained by distributing the molecules according to shape.

We formulate the free energy of a tubule plus surroundings as a function of its radius and composition. Optimality with respect to variation of the radius gives a predicted osmotic pressure difference Δp across the membrane. Optimality with respect to composition predicts the extent to which shape-based redistribution takes place among the molecules. The composition of the principal lipid is calculated to vary by about 7% between the inner and outer monolayers of the tubules. This result reveals a dominant role played by the entropic contribution to the free energy at normal physiological temperatures.

Although our approach does not come close to explaining all aspects of inner membrane morphology, it is well grounded in experimental observations and enables us to leverage observed morphologies into predictions regarding additional aspects of the physico-chemical environment in which membrane morphology is observed.

2. Formulation of the free energy

In this section we formulate the free energy of a tubule and its surroundings as a function of its radius and composition. As indicated in figure 1, the inner mitochondrial membrane is made up of three types of surface. First, those that are approximately flat. These consist of the lamellar shaped cristae and the inner boundary membrane. Mitochondria are about $1 \mu m$ in size. Hence the curvature of the IBM is a few orders of magnitude smaller than that of the tubules; it may also be considered flat. Second, the tubular regions. Third, the crista junctions at which tubular regions connect to the flat ones. In area these three types of surface typically differ by at least an order of magnitude. Most lipids reside in the flat regions. Only a very small fraction forms the crista junctions. Hence, we

neglect in our model the crista junctions. The lipid molecules in the tubules and in the flat regions are in equilibrium. Since the latter constitute a surface of mean curvature approximately zero, the lipid compositions on the two sides (inner and outer) are the same, at least as far as bending forces are concerned. Short of postulating a preference of some lipids for the chemical environment on the two sides of the membrane, we may assume that the compositions on the two sides are the same and act as a reservoir for lipid molecules in the tubular regions. Hence, we consider $N_E^{(*)}$ molecules of DOPE and $N_C^{(*)}$ molecules of DOPC distributed among the inner and outer layers of a cylindrical bilayer of unit length and a flat bilayer reservoir. Let U and S denote respectively the total bending energy and the total entropy of the membrane molecules, and T the temperature. Then, up to constants, the sum of the free energies of all the systems that participate in the energetics of altering the radius of the tubule and its composition can be written as

$$G = U - TS + \Delta p V. \tag{1}$$

In this equation we have dropped the pV term for the membrane and the U and TS contributions of the surrounding cytosol. Thus the $U - TS$ portion is the free energy of the membrane while the ΔpV term is the free energy of the matrix and intermembrane region, which depends on the volume V inside the cylindrical tubule and the osmotic pressure difference Δp between the matrix and intermembrane space, with the higher pressure in the matrix. We will use the following notational conventions. Subscripts E and C will continue to denote the molecular species DOPE and DOPC. Superscripts (i), (o) and (r) will refer, respectively, to the inner and outer monolayers of the tubule, and to either monolayer of the flat bilayer reservoir. N will continue to indicate the number of molecules, and lower case letters u and s will indicate energy and entropy per molecule. More precisely, s will denote a partial molecular entropy. For example, $u_E^{(o)}$ is the partial molecular bending energy of DOPE residing in the outer monolayer of the cylindrical tubule.

Consider first the total bending energy U. The conventional approach is to employ Helfrich's theory [13] and to take the free energy density per unit membrane area as

$$U = \tfrac{1}{2}\kappa_b(C - C_s)^2, \tag{2}$$

where C and C_s are the ambient and spontaneous curvatures of the membrane and κ_b is the bending modulus. However, to allow us to study the lipid redistribution between the monolayers of the tubular membrane and the reservoir, we employ a molecular-level model. Our model takes the bending energy of the bilayer to be additive over the individual lipids in each of the monolayers. Following Israelachvilli [14], we take the bending energy of one lipid molecule in the cylindrical monolayer to be

$$u = \frac{1}{2} K_A a \left(1 - \frac{a_s}{a}\right)^2, \tag{3}$$

where K_A is the compressibility modulus, and a is the characteristic interfacial area of the lipid at the ambient curvature C. The compressibility modulus is related to the bending modulus. For small deformations, κ_b depends linearly

on K_A and quadratically on the membrane thickness [15, 16]. The relation between a and C will be given shortly. For a monolayer containing one type of lipid, a is defined as the area of the membrane divided by the total number of lipids. a_s is the characteristic interfacial area for a monolayer at the spontaneous curvature. Since the spontaneous curvature and hence a_s depend on the type of lipid, the bending energy differs as well. This causes a redistribution over the two leaflets, which represent different ambient curvatures. Spontaneous curvatures have been determined experimentally and are understood as the curvature of 'choice' for a particular lipid type constrained to a cylindrical monolayer with minimum bending energy.

The total bending energy

$$U = N_E^{(i)} u_E^{(i)} + N_C^{(i)} u_C^{(i)} + N_E^{(o)} u_E^{(o)} + N_C^{(o)} u_C^{(o)} + \left(N_E^{(*)} - N_E^{(i)} - N_E^{(o)}\right) u_E^{(r)} + \left(N_C^{(*)} - N_C^{(i)} - N_C^{(o)}\right) u_C^{(r)}. \tag{4}$$

These terms can be rearranged to give

$$U = N_E^{(i)} \Delta u_E^{(i)} + N_C^{(i)} \Delta u_C^{(i)} + N_E^{(o)} \Delta u_E^{(o)} + N_C^{(o)} \Delta u_C^{(o)} + U^{(*)}, \tag{5}$$

where, all four Δ are defined relative to the value of each quantity in the reservoir. For example

$$\Delta u_C^{(o)} = u_C^{(o)} - u_C^{(r)}. \tag{6}$$

We have also defined the quantity

$$U^{(*)} = N_E^{(*)} u_E^{(r)} + N_C^{(*)} u_C^{(r)}, \tag{7}$$

which does not vary as the molecules are redistributed among the three compartments. We introduce $\alpha^{(i)}$ and $\alpha^{(o)}$ to represent the fraction of DOPE on the inner and the outer monolayers of the tubule, respectively. With this, U can be rewritten as

$$U = N^{(i)}\left(\alpha^{(i)} \Delta u_E^{(i)} + (1 - \alpha^{(i)}) \Delta u_C^{(i)}\right) + N^{(o)}\left(\alpha^{(o)} \Delta u_E^{(o)} + (1 - \alpha^{(o)}) \Delta u_C^{(o)}\right) + U^{(*)}. \tag{8}$$

A perfectly analogous formula holds for S:

$$S = N^{(i)}\left(\alpha^{(i)} \Delta s_E^{(i)} + (1 - \alpha^{(i)}) \Delta s_C^{(i)}\right) + N^{(o)}\left(\alpha^{(o)} \Delta s_E^{(o)} + (1 - \alpha^{(o)}) \Delta s_C^{(o)}\right) + S^{(*)}. \tag{9}$$

It remains to formulate the Δs, the N and the Δu. The Δs depend not only on the fractions $\alpha^{(i)}$ and $\alpha^{(o)}$, but also on the fraction $\alpha^{(r)}$ of DOPE in the flat reservoir. Assuming that the membrane contains only DOPE and DOPC and that their ratio is that of the ratio of PE and PC in mitochondrial inner membranes, we have taken $\alpha^{(r)} = \frac{27.7}{27.7+44.5} = 0.384$. We define $\Delta s_E^{(i)}$ and analogous terms to be $s_E^{(i)} - s_E^{(r)}$. The partial molecular entropies are decomposed into a pure part and a mixing part. Since the pure part is the same in all three compartments (i, o, r), the Δs depend only on the mixing, i.e., we write $\Delta s_E^{(i)} = s_{E,\mathrm{mix}}^{(i)} - s_{E,\mathrm{mix}}^{(r)}$.

The total entropy of (ideal) mixing of the two species on the inner monolayer of the tubule is given by

$$S_{\mathrm{mix}}^{(i)} = -k_B N^{(i)}(\alpha^{(i)} \ln \alpha^{(i)} + (1 - \alpha^{(i)}) \ln(1 - \alpha^{(i)})), \tag{10}$$
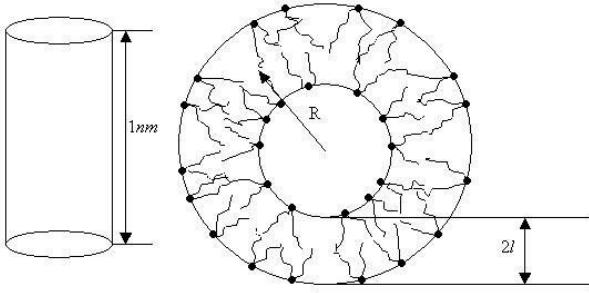
Figure 2. Sketch of a side view and cross section of a tubular part of the membrane. The radius R is measured from the center of the tubule to the middle of the membrane. The thickness of the lipid layer, including only the hydrocarbon tails, is $2l$, to which each monolayer contributes equally.

or, more explicitly, as a function of the molecule numbers

$$S_{\text{mix}}^{(i)} = -k_B \left[N_E^{(i)} \ln \left(\frac{N_E^{(i)}}{N_E^{(i)} + N_C^{(i)}} \right) + N_C^{(i)} \ln \left(\frac{N_C^{(i)}}{N_E^{(i)} + N_C^{(i)}} \right) \right]. \tag{11}$$

The partial molecular entropy is obtained as

$$s_{E,\text{mix}}^{(i)} = \frac{\partial S_{\text{mix}}^{(i)}}{\partial N_E^{(i)}} = -k_B \ln \frac{N_E^{(i)}}{N_E^{(i)} + N_C^{(i)}} = -k_B \ln \alpha^{(i)}. \tag{12}$$

Similarly, $s_{E,\text{mix}}^{(r)} = -k_B \ln \alpha^{(r)}$, and, finally,

$$\Delta s_E^{(i)} = -k_B \ln \frac{\alpha^{(i)}}{\alpha^{(r)}}. \tag{13}$$

The other Δs are obtained similarly

$$\Delta s_E^{(o)} = -k_B \ln \frac{\alpha^{(o)}}{\alpha^{(r)}}, \tag{14}$$

$$\Delta s_C^{(i)} = -k_B \ln \frac{1 - \alpha^{(i)}}{1 - \alpha^{(r)}}, \tag{15}$$

$$\Delta s_C^{(o)} = -k_B \ln \frac{1 - \alpha^{(o)}}{1 - \alpha^{(r)}}. \tag{16}$$

These are now substituted into (9).

The interfacial surface of each compartment (i, o, r) has its own (cylindrical) curvature. They can be expressed in terms of the radius, R, of the midsurface of the cylindrical tubule and the width, l, of the hydrocarbon tails due to one monolayer (see figure 2). It follows that

$$C^{(i)} = \frac{1}{R - l}, \tag{17}$$

$$C^{(o)} = \frac{-1}{R + l}, \tag{18}$$

$$C^{(r)} = 0. \tag{19}$$

For the immediate discussion we suppress the superscripts. Let v be the volume of the hydrocarbon tails of a lipid molecule. Each molecule residing in a cylindrical monolayer with interfacial curvature, C, has a characteristic interfacial area, a, which is defined as the area of the cylindrical tubule divided by the total number of molecules. These quantities are related by the 'packing factor' equation:

$$\frac{v}{al} = 1 + \frac{l}{2}C. \tag{20}$$

In our model the hydrocarbon tails of both lipids are identical and hence $v_E = v_C$, so one a fits all molecules in a monolayer. This means that the total number of molecules in a monolayer can be written as

$$N = \frac{2\pi}{a|C|}. \tag{21}$$

Recall that we take the (fixed) length of the cylindrical tubule to be 1, for convenience. Also recall $C^{(o)}$ is negative; hence, the absolute value. Combining (20) and (21), we have

$$N = \frac{2\pi l}{v|C|} \left(1 + \frac{l}{2}C \right). \tag{22}$$

Using (17) and (18) to adapt (22) to the two cylindrical monolayers, we have

$$N^{(i)} = \frac{\pi l}{v}(2R - l). \tag{23}$$

$$N^{(o)} = \frac{\pi l}{v}(2R + l). \tag{24}$$

We now calculate the following bending energies:

$$u_E^{(i)}, \quad u_E^{(o)}, \quad u_E^{(r)}, \quad u_C^{(i)}, \quad u_C^{(o)}, \quad u_C^{(r)}. \tag{25}$$

Combining (3) and (20), we obtain

$$u = \frac{1}{2} K_A a_s \frac{(C - C_s)^2}{(2/l + C_s)(2/l + C)}. \tag{26}$$

Distributing the appropriate subscripts and superscripts to the quantities u, K_A, C and C_s, we obtain the six quantities (25). This completes the formulation of the free energy G.

Values for all constants have been obtained from the literature. The thickness of the layer of hydrocarbon tails, l, is assumed to be constant in the model at hand and equals 1.6 nm [14]. Experimentally it has been found that, when DOPE and DOPC form monolayers with a cylindrical shape, their spontaneous curvatures, C_s, are the inverse of their intrinsic radii of curvature respectively $1/2.06 \text{ nm}^{-1}$ and $1/9.05 \text{ nm}^{-1}$ [17]. The area per headgroup a_s for DOPE equals 0.163 nm^2 [14]. Using (20) for DOPE one obtains $v = 0.362 \text{ nm}^3$. Since the volume of the hydrocarbon tails of the two lipid species is the same, one can use the same formula (20) to obtain that a_s for DOPC equals 0.208 nm^2. The compressibility moduli for DOPE and DOPC are $33.0 \, k_B T \text{ nm}^{-2}$ and $26.4 \, k_B T \text{ nm}^{-2}$, respectively [18].

3. Results and discussion

For values of Δp between 0.4 mbar and 4 bar, the free energy G as a function of the radius R and the compositions $\alpha^{(i)}$ and $\alpha^{(o)}$ have been calculated using (1). Figure 3 gives the free energy as a function of R for a pressure difference $\Delta p = 0.005 \, k_B T \text{ nm}^{-3}$ (0.2 bar) and compositions of monolayers of the tubular membrane given by $\alpha^{(i)} = 0.423$ and $\alpha^{(o)} = 0.352$. These values for $\alpha^{(i)}$ and $\alpha^{(o)}$ yield the lowest free energy; changing the compositions of the monolayers results in a similar graph to that shown in figure 3, except that the value of $G/k_B T$ at which a minimum occurs is higher. Figure 3 shows the total free energy as well as the individual contributions of entropy and bending energy of the membrane, and the free
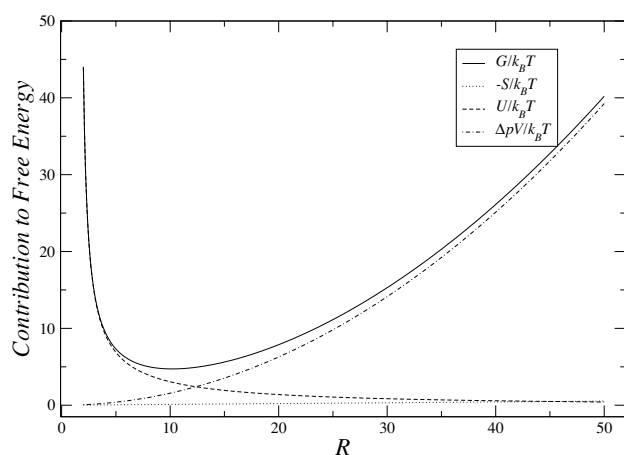
Figure 3. Free energy as function of radius R at $\Delta p = 0.005 \, \mathrm{k}_B T \, \mathrm{nm}^{-3}$, $\alpha^{(i)} = 0.423$ and $\alpha^{(o)} = 0.352$. The contributions of the different terms in (1) are shown independently.

Table 1. Values of the minimum free energy as a function of the pressure difference, along with the optimum values for R, $\alpha^{(i)}$ and $\alpha^{(o)}$.

Δp ($\mathrm{k}_B T \, \mathrm{nm}^{-3}$)	Δp (bar)	R (nm)	G ($\mathrm{k}_B T$)	$\alpha^{(i)}$	$\alpha^{(o)}$
0.00001	0.0004	72.8	0.6	0.388	0.379
0.0001	0.004	35.6	1.2	0.393	0.374
0.001	0.04	16.7	2.6	0.405	0.364
0.005	**0.2**	**9.9**	**4.4**	**0.423**	**0.352**
0.01	0.4	8.0	5.6	0.433	0.347
0.02	0.8	6.5	7.2	0.448	0.341
0.03	1.2	5.8	8.4	0.458	0.336
0.04	1.6	5.3	9.3	0.474	0.331
0.05	2.0	5.0	10.1	0.477	0.329
0.07	2.8	4.6	11.5	0.486	0.327
0.1	4.0	4.2	13.3	0.499	0.323

energy of the surroundings. The scale is arbitrary and set so that the free energy vanishes at infinite R, zero Δp and $\alpha^{(i)} = \alpha^{(o)} = \alpha^{(r)}$. The pressure difference (0.2 bar) is adjusted such that the free energy curve has a minimum at $R = 9.9$ nm, which is close to the experimentally observed value. The pressure difference corresponds to a concentration difference of 8 mM.

Setting our scale in figure 3 so as to make the free energy vanish at infinite R, zero Δp and $\alpha^{(i)} = \alpha^{(o)} = \alpha^{(r)}$ amounts to setting the quantities $U^{(*)}$ in (8) and $S^{(*)}$ in (9) to zero. Their values are independent of R, $\alpha^{(i)}$ and $\alpha^{(o)}$. Setting them to zero will not change the location of the minimum of free energy. It follows that all three terms in (1) scale linearly with the length of the tubule. Therefore, our results are valid for arbitrary length.

At each value of Δp, the free energy was minimized and the results are tabulated in table 1 which lists values of R, $\alpha^{(i)}$ and $\alpha^{(o)}$, that minimize the free energy G, for various values of the pressure difference. Figure 4 shows how R varies as a function of Δp along this locus of minimum free energy. Interestingly, the radius of 10 nm is reached in the 'elbow' of the curve. Increasing the pressure by one order of magnitude decreases the radius by half. However, decreasing the pressure by one order increases the radius by a factor of
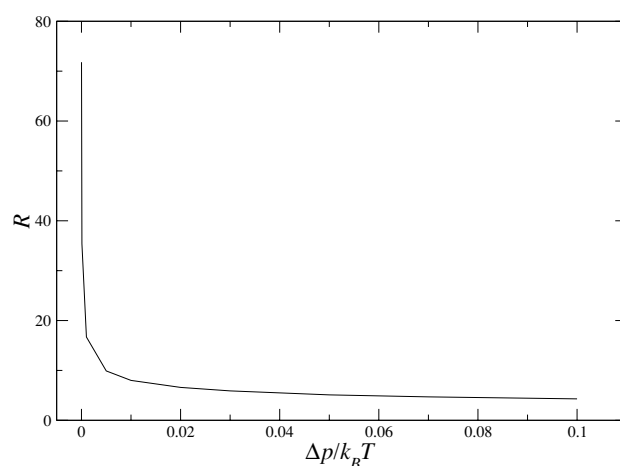

Figure 4. Radius as a function of pressure difference. $\Delta p = 0.025 \, \mathrm{k}_B T \, \mathrm{nm}^{-3}$ corresponds to a pressure difference of 1 bar.
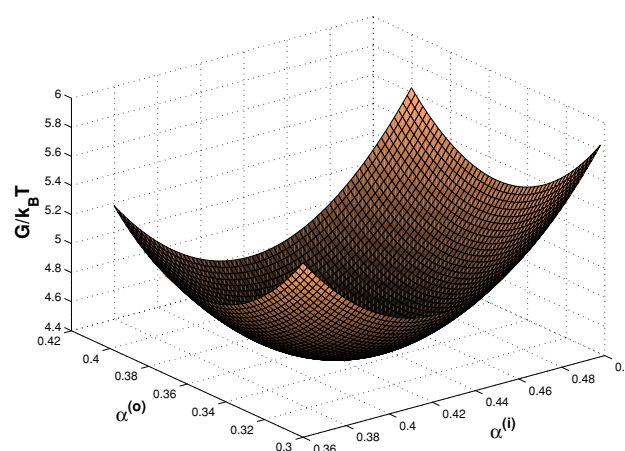

Figure 5. Free energy as a function of $\alpha^{(i)}$ and $\alpha^{(o)}$. The radius of the tubule $R = 9.9$ nm, and $\Delta p = 0.005 \, \mathrm{k}_B T \, \mathrm{nm}^{-3}$.

five or so. As expected, the value of the free energy decreases with increasing radius. It will be zero at infinite radius and zero pressure difference. At these values, $\alpha^{(i)} = \alpha^{(o)} = \alpha^{(r)}$. At a finite pressure, more DOPE than average is found in the inner layer and more DOPC in the outer layer. At the highest pressure difference $\Delta p = 0.1 \, \mathrm{k}_B T \, \mathrm{nm}^{-3}$ (4 bar) the fraction of DOPE differs by 0.18 between the two layers of the tubule.

Figure 5 shows the variation of the free energy as a function of lipid distribution. A sharp increase in free energy can be observed when the composition deviates from its optimum at $\alpha^{(i)} = 0.423$ and $\alpha^{(o)} = 0.352$.

A weakness of the current approach is that the Helfrich energy (2) is only valid for small deviations from the spontaneous curvature. Curvatures of the inner and outer monolayers of the tubules differ by up to 100% from the spontaneous curvatures. It follows that (3) is only approximately valid. Currently, we are performing Monte Carlo simulations in the hope of obtaining the higher-order corrections to this equation. Using these in the calculations will improve the results as will adding the effects of other

membrane components on the spontaneous curvature and on the elastic moduli.

4. Conclusion and outlook

In this paper we have considered a two-lipid model of the inner mitochondrial membrane and examined the changes in free energy for the tubular parts caused by variations in shape and composition. The analysis led to two predictions: (1) the observed radius of 10 nm implies that there is a 0.2 atmosphere osmotic pressure difference across the inner membrane, with the higher pressure in the matrix and (2) lipids redistribute themselves to give different compositions on the two sides of the tubular membrane, since the resulting decrease in bending energy is smaller than the entropic penalty. Using our model, we found that for crista tubules of the observed size the lipid compositions on the two sides of the membrane differ by about 7%. Although the possibility that composition drives shape changes have been discussed before [8, 10], most theoretical approaches in the literature neglect a composition dependence. Recent neutron diffraction measurements on mixed DOPE/DOPC monolayers in the inverted hexagonal phase have found that the more cone-shaped DOPE lipids accumulate in the areas of highest curvature [9]. In agreement with our findings, they show that this effect is significant. If we were to neglect composition variations the predicted osmotic pressure difference would increase 12%. We plan to extend our calculations to the crista junctions. They have the most extreme curvature, so one would expect an even stronger separation of the lipid components in reaching the free energy minimum.

The 2-lipid model neglects the numerous components, besides DOPE and DOPC, that reside in the inner mitochondrial membrane. The presence of these components in the membrane will influence the predicted values of the pressure difference and composition. Hence, we also plan to obtain the bending energy from measurements on swollen mitoplasts. Inserting the measured value of the bending modulus κ_b in formula (2) for the Helfrich energy will yield a value for the bending energy that accounts for all membrane components including cardiolipin and high concentrations of a variety of integral membrane proteins.

Our model predicts that changes in the radii of tubules and junctions correspond to variations in pressure difference. This might be tested experimentally by manipulating the osmotic pressure in preparations of purified mitochondria and observing changes in the radii of tubular components. It has been suggested that the junctions act as a barrier to the diffusion of cytochrome c. Indeed Scorrano *et al* [19] have observed that during apoptosis the inner membrane remodels, and the radii of the tubules increase. In certain types of mitochondria, they can increase in these *in vitro* experiments to 20 nm. As seen in table 1, this corresponds, according to our model, to a large change in the osmotic pressure difference. On the other hand, purified mitochondria that have been induced to undergo a permeability transition in buffer of low osmolarity experience an increased Δp that causes the matrix to swell.

The crista junctions in these mitochondria are slightly smaller with radii of 8.5 nm [7].

Although the model at hand successfully describes some of the features of the observed morphology, it fails to explain some crucial issues. For instance, as can be seen in figure 3, the minimum value of the free energy for tubules is positive and hence these structures are predicted to be unstable. Additional mechanisms must be at work that prevent them from shrinking and vanishing in the flat membrane regions. One possibility is that such a mechanism is provided by proteins and skeletal elements. However, we can envision an alternative mechanism. Since the inner membrane is confined by an outer one, the area can grow only by buckling or by creating protrusions. It is very likely that the confinement causes tensile stresses. Currently we are investigating the possibility that, thermodynamically, the combined effects of osmotic pressure differences and tensile stresses account for the observed coexistence of cylindrical tubes of finite radius and flat lamellar structures. In addition, since the membrane is fluid, tubules will continuously arise, grow, shrink and eventually vanish back into the flat portions of the membrane. It is quite likely that not just the structural organization of mitochondria, but also temporal variations of this structure, is of importance for understanding mitochondrial functionality.

Acknowledgments

Glossary

Apoptosis. A programmed or controlled form of cell death.

Bending energy. Work required to change the curvature of a membrane from its spontaneous curvature.

Crista. An infolding of the inner mitochondrial membrane, that projects into the matrix.

Matrix. The compartment enclosed by inner mitochondrial membrane.

Mitoplast. The mitochondrial inner membrane and matrix, following removal of the outer membrane.

References

[1] Frey T G and Manella C A 2000 *Trends Biochem. Sci.* **25** 319–24

[2] Frey T G, Renken C S and Perkins G A 2002 *Biochim. Biophys. Acta* **1555** 196–203

[3] Perkins G A and Frey T G 2000 *Micron* **31** 97–111

[4] Renken C, Siragusa G, Perkins G, Washington L, Nulton J, Salamon P and and Frey T G 2002 *J. Struct. Biol.* **138** 137–144

[5] Lipowski R and Sackmann E ed. 1995 *Handbook of Biological Physics* vol 1 (Amsterdam: Elsevier)

[6] Hackenbrock C R 1968 *Proc. Natl Acad. Sci. USA* **61** 598–605
[7] Renken C 2004 The structure of mitochondria *PhD Dissertation* San Diego State University
[8] Gozdz W T and Gompper G 1998 *Phys. Rev. Lett.* **80** 4213–6
[9] Ding L, Weiss T M, Fragneto G, Liu W, Yang L and Huang H W 2005 *Langmuir* **21** 203–10
[10] Julicher F and Lipowsky R 1993 *Phys. Rev. Lett.* **70** 2964
[11] Baumgart T, Hess S T and Webb W W 2003 *Nature* **425** 821–4
[12] Tsafrir I, Sagi D, Arzi T, Gueseau-Boudeville M, Frette V, Kandel D and Stavans J 2001 *Phys. Rev. Lett.* **86** 1138-41
[13] Helfrich W 1973 *Z. Naturforschr.* C **28** 693–703

[14] Israelachvili J N 1995 *Intermolecular and Surface Forces* (San Diego, CA: Academic)
[15] Landau L D and Lifshitz E M 1986 *Theory of Elasticity* (Oxford: Pergamon)
[16] Boal D 2002 *Mechanics of the Cell* (Cambridge: Cambridge University Press)
[17] Steicher-Scott J, Lapidus R and Sokolove P M 1994 *Arch. Biochem. Biophys.* **315** 548–54
[18] Fuller N and Rand R P 2001 *Biophys. J.* **81** 243–54
[19] Scorrano L, Ashiya M, Buttle K, Weiler S, Oakes S A, Mannella C A and Korsmeyer S J 2002 *Dev. Cell.* **2** 55–67